

## Subchronic memantine induced concurrent functional connectivity and altered ultra-structural tissue integrity in the rodent brain: revealed by multimodal MRI

Sekar S<sup>1,2,\*</sup>, Jonckers E<sup>1</sup>, Verhoye M<sup>1</sup>, Willems R<sup>2</sup>, Veraart J<sup>3</sup>, Van Audekerke J<sup>1</sup>, Couto J<sup>4</sup>, Giugliano M<sup>4</sup>, Wuyts K<sup>5</sup>, Dedeurwaerdere S<sup>6</sup>, Sijbers J<sup>3</sup>, Mackie C<sup>5</sup>, Ver Donck L<sup>2</sup>, Steckler T<sup>2</sup>, Van der Linden A<sup>1</sup>

**1** Bio-Imaging Lab, **3** Vision Lab, **4** Theoretical neurobiology, **6** Translational Neuroscience, University of Antwerp,

**2** Neuroscience Discovery, **5** ADME/Tox, Janssen Research & Development, Belgium.

**Disclosure:** This manuscript is the peer-reviewed version of the article

Sekar S, Jonckers E, Verhoye M, Willems R, Veraart J, Van Audekerke J, Couto J, Giugliano M, Wuyts K, Dedeurwaerdere S, Sijbers J, Mackie C, Ver Donck L, Steckler T, Van der Linden A.

Subchronic memantine induced concurrent functional connectivity and altered ultra-structural tissue integrity in the rodent brain: revealed by multimodal MRI. *Psychopharmacology (Berl)*.  
2013 Jun;227(3):479-91. doi: 10.1007/s00213-013-2966-3. The final publication is available at

<http://link.springer.com/article/10.1007%2Fs00213-013-2966-3>

### Corresponding Author:

Dr. Sakthivel Sekar, PhD

Bio-Imaging Lab; Department of Biomedical Sciences; Campus Drie Eiken; D.UC.109;  
University of Antwerp, Universiteitsplein 1; 2610 Wilrijk; Belgium  
Telephone: (+32) 3 265 2775; Fax: (+32) 3 265 2774  
Email: [sekar.sakthivel@ua.ac.be](mailto:sekar.sakthivel@ua.ac.be)

**ABSTRACT:**

**Background:** An effective NMDA antagonist imaging-model may find key utility in advancing schizophrenia drug discovery research. We investigated effects of sub-chronic treatment with the NMDA antagonist memantine using behavioural observation and multimodal MRI.

**Methods:** Pharmacological MRI (phMRI) was used to map the neuroanatomical binding sites of memantine after acute and sub-chronic treatment. Resting state fMRI (rs-fMRI) and diffusion MRI were used to study the changes in functional connectivity (FC) and ultra-structural tissue integrity before and after sub-chronic memantine treatment. Further corroborating behavioural evidences were documented.

**Results:** Dose-dependent phMRI activation was observed in the prelimbic cortex following acute doses of memantine. Sub-chronic treatment revealed significant effects in the hippocampus, cingulate, prelimbic and retrosplenial cortices. Decreases in FC amongst the hippocampal and frontal cortical structures (prelimbic, cingulate) were apparent through rs-fMRI investigation, indicating a loss of connectivity. Diffusion kurtosis MRI showed decreases in fractional anisotropy and mean diffusivity changes suggesting ultra-structural changes in the hippocampus and cingulate cortex. Limited behavioral assessment suggested that memantine induced behavioral effects comparable to other NMDA antagonists as measured by locomotor hyperactivity, and that the effects could be reversed by antipsychotic drugs.

**Conclusion:** Subsequent adaptations in phMRI results and decreases in FC are indicative of ultra-structural changes following sub-chronic memantine treatment. These changes may underlie the behavioural effects. The present findings underscore the utility of memantine and multimodal-MRI in the search for novel disease-modifying treatments for schizophrenia.

**Keywords:** NMDA antagonists, memantine, locomotor activity, pharmacological MRI, resting state-fMRI, DTI/DKI, cingulate cortex, hippocampus, schizophrenia, antipsychotic drugs.

**1 INTRODUCTION:**

In vivo translational imaging, such as magnetic resonance imaging (MRI) and positron emission tomography (PET), has gained substantial interest in advancing drug discovery research (Fox et al. 2009; Wong et al. 2009). Functional, resting-state and diffusion imaging are specialized MRI protocols particularly useful in CNS drug discovery research. While functional magnetic resonance imaging (fMRI) is extensively used to investigate central activity related to sensory or cognitive stimuli, a blood oxygenation level dependent (BOLD) fMRI response can also be evoked when the brain is challenged by psychoactive compounds (Borsook et al. 2006). This technique is commonly referred to as pharmacological MRI (phMRI) (Borsook & Becerra, 2010). Resting state fMRI (rs-fMRI), on the other hand, has the potential to investigate functional connectivity (FC) in the pharmacologically modulated brain in rodents (Bifone et al. 2010; Schwarz et al. 2007). Similarly diffusion kurtosis imaging is particularly useful in characterising the ultra-structural tissue changes in disease models (Delgado y Palacios et al. 2011).

These neuro-imaging methods therefore allow a better understanding of the neurobiological mechanisms underlying psychoactive drug effects. Briefly mapping the neuroanatomical target sites and studying the subsequent adaptations across doses, treatment regimes and/or with a co-administration of a suitable agonist or antagonist allows for a better understanding of the mechanism of action of compounds in-vivo (Sekar et al. 2010, 2011(a, b)).

The glutamatergic hypothesis of schizophrenia is supported by several lines of clinical evidence; this includes post-mortem, genetic and human psychosis modelling (Krystal et al. 1994; Malhotra et al. 1997). In this context, NMDA antagonists, such as ketamine or phencyclidine (PCP), can induce a wide range of positive, negative and cognitive symptoms in healthy volunteers that resemble those in patients with schizophrenia (Coyle & Tsai, 2004; Mechri, et al. 2001-a). When administered to patients, the exacerbated psychotic symptoms have a striking similarity to the symptoms during their usual schizophrenic episodes (Bubeníková-Valesová et al. 2008; Mechri et al. 2001-a, b).

Using in-vivo phMRI, Gozzi et al. (2008-a) investigated the modulatory effects of PCP along with co-treatment by endogenous and exogenous agonists on the BOLD signal in rats. Ketamine was reported to produce a dose-dependent increase in the BOLD-MR signal localized in the frontal, hippocampal, cortical and limbic areas, which correlated with the pharmacodynamic profile of the drug (Littlewood et al. 2006-a). In a parallel study involving stereo-isomers of ketamine [(R-), (S+)], comparable activation was observed in cortical and hippocampal regions (Littlewood et al. 2006-b). Further studies in humans using [18F]-fluorodeoxyglucose and PET imaging showed that a sub-anaesthetic dose of ketamine induced a bilateral increased metabolic activity in regions of the prefrontal cortex (Langsjo et al. 2004) and a reduced cerebral blood flow in the hippocampus (Mechri et al. 2001-a; Langsjo et al. 2003; Langsjo et al. 2004). Similar responses have been reported using the NMDA antagonist MK-801 in the limbic and frontal cortex in a phMRI study; this correlated with changes in 2-deoxyglucose (2-DG) autoradiography of regional brain glucose metabolism in rats (Houston et al. 2001).

Memantine is a low affinity, high voltage-dependent non-competitive antagonist of the NMDA receptor; it has fast blocking-unblocking kinetics, which facilitates a rapid clearance from the NMDA channel during physiological activation, yet blocking the receptors during peak activity (Danysz et al. 2000). Earlier work demonstrated robust and reproducible increases in brain glucose metabolism after acute memantine treatment in mice, and this effect was reversible with antipsychotic drugs (Dedeurwaerdere et al. 2011).

Despite profound differences in pharmacokinetics, behavioural profiling of memantine in rats has demonstrated similar disruptions in spontaneous and reward-motivated psychomotor behaviours between ketamine and memantine (Gilmour et al. 2009). However ketamine has been classified as a controlled drug and PCP was withdrawn from the clinical formulary because of abuse liability and neurotoxicity concerns (Olney et al. 1991, 1995); whereas memantine is safely used in the clinic, to improve cognitive function in Alzheimer's patients (Peskind et al. 2006; Winblad et al. 2007). Memantine is well tolerated, has linear kinetics and 100% bioavailability (following oral dosing) (Aerosa et al. 2005; Wilcock et al. 2002). Moreover an advantage of memantine compared to ketamine is its long biological half-life known to be around 2-4 h (Alley et al. 2010). Hence an MRI imaging model using memantine would be

useful to explore novel disease modifying treatments across pre-clinical and clinical settings *in-vivo*. To our knowledge, this is the first multimodal imaging study investigating memantine in rats.

The aim of this study was i) to evaluate the effects of acute and sub-chronic administration of memantine on brain activation as well as functional and anatomical connectivity using multimodal imaging techniques in rats and ii) to correlate these with behavioural responses. We have used phMRI to map the neuroanatomical target sites of memantine and to study the subsequent adaptation in the BOLD response from acute to sub-chronic treatment. rs-fMRI was used to study FC among discrete brain structures apparent from the phMRI results. Finally, diffusion MRI was used to study the ultrastructural changes in the regions of interest.

## **2 METHODS and MATERIALS:**

### **2.1 ANIMALS:**

All procedures were conducted in compliance with Belgian law (Royal Decree on the protection of laboratory animals dd. April 6, 2010). The study protocols were approved by the institutional animal experimental ethical committees of Janssen Research & Development (Beerse, Belgium) and University of Antwerp (Antwerp, Belgium).

Male Lister Hooded rats were obtained from Charles River (Germany). Animals were housed in enriched individual ventilated cages (IVC) in groups of 4 and habituated to environmental conditions for at least 5 days with food and water *ad libitum* (conditions: 12:12 h light/dark cycle, temperature, 20-24° C and humidity 45-65%). Mean body weight range at experimental day was 240-300 gram. Rats were used only once in an experiment and euthanized afterwards.

### **2.2 DRUGS and TREATMENT GROUPS:**

#### **2.2.1 Behavioural experiments:**

Memantine was obtained from Manus Aktteva Biopharma (Ahmedabad, India); PCP, risperidone, haloperidol and olanzapine were synthesised at Janssen Research & Development (Beerse, Belgium). In the acute dose-response experiments, memantine or PCP was administered at doses of 10, 20 or 40 mg/kg IP or 0.63, 1.25 or 2.5 mg/kg subcutaneously (SC) respectively.

Based on the inference from these acute dose-response experiments and from the historical data from studies in Janssen Research & Development, subjects received memantine (20 mg/kg/day, IP) or PCP (1.25 mg/kg/day, SC) once daily for five consecutive days. Two to three days after the last sub chronic administration, rats were challenged acutely with memantine (20 mg/kg, IP) or PCP (2.5 mg/kg, SC) respectively. Saline was used as the vehicle to dissolve memantine or PCP. Haloperidol was dissolved in saline + 1 equivalent tartaric acid (=0.5 ml of 1N tartaric acid per 10 mg compound); olanzapine and risperidone were dissolved in saline + 2 equivalents tartaric acid. Vehicle was administrated in the control group. Drugs were administered 30 min prior to acute challenge with memantine or PCP. All compound solutions were stored at room temperature in a closed container protected from light and injection volume was 10 ml/kg. The study involved 49 experimental groups: n = 10 rats/group in acute and in sub-chronic memantine or PCP experiments, n = 12 rats/group in antipsychotic drug testing experiments. The experimental design of the behavioural experiments is provided in Table 1 (see suppl. material).

### **2.2.2 Imaging experiments:**

Acute phMRI experiments involved memantine administered in two doses (20 and 40 mg/kg IP). For sub-chronic testing, single daily injections of 20 mg/kg/day (IP) was used for five consecutive days. Saline was used as the vehicle, for all preparations. Dose selection was based on our behavioural data and a previously published dose-response study, to evaluate NMDA antagonist-induced 2-DG functional brain activations (Dedeurwaerdere et al. 2011).

It is worth mentioning that memantine has been safely used in the clinic; however the therapeutic doses are in the order of at least five times lower than the 20 mg/kg dose utilized in this study (Parsons et al. 2007).

Study design and overview of the imaging experiments are provided in Table 2. Overview of the scanning experimental design and time points are provided in Figure 1(a & b). For phMRI measurements, the study involved five experimental groups (n=6 rats in each group): acute memantine treatment dose-1, dose-2, controls (vehicle treated), sub-chronic memantine treatment (20 mg/kg, IP), chronic control (vehicle treated).

For all phMRI experiments, a single IP administration of memantine or saline was used as the stimulus to generate a phMRI-BOLD response. Longitudinal resting-state or diffusion MRI measurements were conducted before and after sub-chronic treatment in separate groups of 8 or

10 rats, respectively. In addition, diffusion measures were acquired after 3 days of wash out. No drug/vehicle challenge was involved in the resting-state and diffusion MRI measurements, as compared to pHMRI measurements.

### **2.2.3 Pharmacokinetics experiments:**

Pharmacokinetics of memantine were determined in plasma and brain after acute and sub-chronic treatment to correlate with responses in the MRI and behavioural studies. A single or 5 day repeated injection of memantine (20 mg/kg, IP) was given to treatment naïve animals (n=3/group) and subjects were sacrificed at 0.5, 1, 2, 4, 7, 24 h post-dose to collect blood and brain samples.

## **2.3 LOCOMOTOR ACTIVITY:**

### **2.3.1 Apparatus**

Locomotor activity (LMA) was measured by placing rats in black perspex cylinders of Ø 30 cm and 35 cm height with infra-red light provided via the open circular area at the bottom. Live images captured by a CCD-video camera (5 frames/sec) mounted 50 cm above each cylinder (12 in total) enabled image analysis software (Ethovision XT, Noldus, The Netherlands) to quantify total distance travelled: tracking areas for each cylinder were individually calibrated and the X-Y coordinates of the centre of gravity of each subject as determined by the software per video frame was used to calculate total distance travelled. All experiments were performed during the light cycle, between 8:00 and 17:00.

### **2.3.2 Experimental procedure & data analysis:**

Animals were placed in the arenas for a 30 min habituation phase followed by 60 min after administration of an acute challenge with memantine, PCP or their vehicle. Total distance travelled was cumulated over the habituation and challenge periods respectively. Ethovision data were exported to MS Excel for graphing and imported in SPSS (IBM, US) for statistical analysis by unpaired t-test or ANOVA with Dunnett's post hoc test as appropriate.

## **2.4 MULTIMODAL MRI IMAGING:**

### **2.4.1 Subject preparation:**

Initially, rats were anesthetized with 3.5% isoflurane (Isoflo®, Abbot Laboratories Ltd., USA) in a gas mixture of 200 ml/min oxygen and 300 ml/min nitrogen in an induction-box, an IP catheter was placed for the drug challenge and positioned in a stereotaxic head-holding device as described previously (Sekar et al. 2011(a,b)). During phMRI or diffusion MRI data acquisition, maintenance of the anaesthesia was achieved using 0.9 to 2% isoflurane. For the rs-fMRI experiment, the use of isoflurane is argued to be suboptimal (Williams et al. 2010), hence animals were sedated using medetomidine (Domitor, Pfizer, Germany), which has been reported to preserve functional connectivity (Pawela et al. 2009). Initially a bolus of 0.05 mg/kg was injected SC and isoflurane was discontinued after 5 min; followed by a continuous infusion of medetomidine (0.1 mg/kg/h, SC). After the scanning procedure, medetomidine was antagonized by an injection of atipamezole (0.1 mg/kg, SC) (Antisedan, Pfizer, Germany) (Weber et al. 2006).

Uninterrupted physiological monitoring and maintenance was observed throughout the experiments, as described in Sekar et al (2011-a,b). Subject selection for scanning was counterbalanced across treatment/dosing groups, to have an even distribution across day-light time. Repeated scanning sessions in the same animal were planned taking into account the diurnal rhythm.

#### **2.4.2 Experimental protocol:**

All imaging experiments were performed on a 9.4T Biospec scanner (Bruker, Ettlingen, Germany) using a Bruker linear transmit volume coil. An actively decoupled circular-surface receiver coil was placed on top of the stereotactically-positioned flat skull of the rat. For rs-fMRI a parallel receive surface array was used.

PhMRI images were acquired using a gradient echo sequence (TR: 1048 ms, TE: 17 ms, FOV: (25x25) mm<sup>2</sup>, Matrix size: 64x64, Slice thickness: 0.5 mm, 32 axial slices, resolution: (0.39x0.39x0.5) mm<sup>3</sup>. Hundred-twenty functional scans were acquired for each subject: 30 baseline (33 min) and 90 post-injection (100 min) scans (Figure 1).

For rs-fMRI a single shot gradient echo EPI sequence was used to obtain the images (TR: 2000 ms, TE: 16 ms, FOV: (30x30) mm<sup>2</sup>, matrix size: 128x128, Slice thickness: 1 mm, 12 axial slices, resolution: (0.23x0.23x1) mm<sup>3</sup>, bandwidth 400 kHz, 150 repetitions).

Diffusion MRI images were acquired using an SE-EPI sequence (TR: 10 s, TE: 24 ms, FOV: (35x23) mm<sup>2</sup>, acquisition matrix: 96x64, zero filled to 128x64, 50 axial slices, resolution: (0.28x0.37x0.5) mm<sup>3</sup>). Diffusion weighted images were acquired with diffusion gradient pulse duration ( $\delta$ ) = 5 ms, diffusion gradient separation ( $\Delta$ ) = 12 ms, and b values 500, 1000, 2800 s/mm<sup>2</sup> applied in 33, 88, 178 noncollinear optimized directions, respectively.

### 2.4.3 Data analysis:

#### 2.4.3.1 Pharmacological MRI:

Prior to statistical analysis, images were extensively pre-processed. The image time series from each subject was realigned using a least-square approach and rigid body spatial transformation to eliminate any potential motion related artefacts using SPM99. A single subject (from the experimental group) was randomly chosen as the template and all subjects were spatially normalized to the template using a 12 parameter affine transformation. BOLD changes from large blood vessels were limited from the subsequent analysis by masking all pixels with a temporal coefficient of variance greater than 15% (Hlustik et al. 1998); thereby minimising the contamination of surrounding parenchyma associated with spatial smoothing. Individual brain masks, generated using AMIRA software (Visage Imaging), were subsequently applied to each subjects' time series, which were Gaussian smoothed to impose a normal distribution, using a full width half maximum (FWHM) kernel of 0.78x0.78x1 mm<sup>3</sup> (twice the size of image resolution). A comparison between pre- and post-injection scans ("off/on" model) was used to assess the main effect of the treatment and parametric maps of statistical significance were obtained using a fixed effects general linear model, using SPM99, as previously described (Sekar et al. 2011 (a, b)). Relative longer half-life of memantine compared to other NMDA antagonists (Alley et al. 2010) ensure elevated memantine concentrations for the duration of the imaging experiment. A comparison of pre- and post-injection scans serves to be a suitable method of assessing the phMRI-BOLD responses. Global muscle signal intensities were determined for each subject and used as covariates, controlling for global drift effects (Lowe et al. 2008). Subject movement was considered by including the realignment parameters as a nuisance variable (covariates of no interest). Statistical significance for the SPMs was set at p<0.05, corrected for multiple comparisons (using a random gaussian field (RGF) method, a statistically

valid approach that would not be hobbled by the overly conservative assumptions of a standard Bonferroni correction). Group statistical parametric map for each treatment (overlaid onto anatomical structural images) displaying T-distribution of BOLD contrast changes after drug administration, with coloured pixels representing T-scores of significant increases and decreases between 'pre' and 'post' scans were determined. General linear model univariate analysis of variance between subjects' mean muscle signal intensities and injection protocol was determined, to investigate the systemic effect components in the data (Lowe et al. 2008).

#### **2.4.3.2 Resting state fMRI:**

Prior to FC assessment an equally comparable/extensive pre-processing (as with the phMRI analysis) was conducted on the rs-fMRI data, using SPM8: including realignment, normalization, estimation of nonlinear deformations, matching and in plane smoothing using an 0.4-mm Gaussian filter (FWHM) (Jonckers et al. 2011). A band pass filter (0.01 Hz-0.1 Hz) was applied to the temporal data to rule out low frequency noise. To calculate the functional connectivity, region of interest (ROI)-based analysis was conducted, using 'resting-state fMRI data analysis toolkit' (REST). ROI's selection was based on the results of the pharmacological MRI. ROI delineations was performed using AMIRA in accordance to the standard Paxinos rat brain atlas (Paxinos, Watson, 1982). A correlation matrix was calculated displaying the FC between the regions identified as primary regions of interest by the sub-chronic phMRI study, including prelimbic cortex, cingulated cortex and the hippocampus. Moreover the FC between left and right striatum was assessed as a control, were no changes due to treatment were predicted. For all calculations motion correction was applied, significantly improving the FC calculations (Kalthoff et al. 2011). Effect of sub-chronic memantine treatment was assessed by comparing correlation values in SPSS16.0 (<http://www.spss.com/software/statistics/>) using a repeated measurements design for a  $p<0.05$ .

#### **2.4.3.3 Diffusion MRI:**

Prior to diffusion MRI analyses, each diffusion-weighted data was corrected for potential subject motion as well as geometrical eddy current distortions by affinely aligning all diffusion-weighted images to a non-diffusion-weighted reference image. Next, the diffusion gradient directions were

rotated correspondingly to preserve the orientation information of the diffusion-weighted data (Leemans & Jones 2009).

More reproducible and consistent delineation of ROIs for further statistical analyses of the diffusion MRI data was facilitated by warping all subjects nonlinearly to a study-specific population-based reference template. To this end, all diffusion weighted data were initially normalized to an arbitrarily chosen reference dataset by in-house affine coregistration software based on the maximization of the mutual information (Maes et al. 1997). Residual local image misalignments were afterwards corrected by warping all subjects onto a study-specific population-based diffusion tensor imaging (DTI) atlas using a non-rigid co-registration technique, based on a viscous fluid model (Van Hecke et al. 2008).

In this study, the diffusion kurtosis model was voxel-wise fitted to the normalized diffusion weighted images to allow a more accurate estimation of the Gaussian, as well as the non-Gaussian diffusion of water molecules (Veraart et al. 2011). A weighted least squares estimator was used to get an estimate of the diffusion tensor and diffusion kurtosis tensor, which quantify the apparent diffusion coefficient and the deviation from Gaussian diffusion, respectively (Jensen et al. 2005). From the tensor information diffusion parameters [fractional anisotropy (FA), axial-(AD), radial- (RD) & mean-diffusivity (MD)] and additional diffusion kurtosis parameters [mean- (MK), axial- (AK) & radial-kurtosis (RK)] were calculated; subsequently repeated measures ANOVA and paired-sample t-test were conducted to test for the treatment effect for the different diffusion parameters.

## 2.5 PHARMACOKINETICS OF MEMANTINE

Subjects were sacrificed at the pre-defined time points (0.5, 1, 2, 4, 7, 24 h post-dose) by decapitation and blood was collected by exsanguination. The whole brain was rapidly dissected and immediately stored at  $\leq -18^{\circ}\text{C}$ . Plasma was obtained following centrifugation at  $4^{\circ}\text{C}$ . After thawing, brain samples were homogenized in demineralised water (1/9 w/v), under dimmed light conditions. Memantine concentrations in plasma and brain homogenates were analysed by the Bioanalytical Department (Janssen R&D, Beerse, Belgium) using a qualified research high-performance liquid chromatography with tandem mass spectrometric (LC-MS/MS) detection method. The lower limit of quantification was 2.0 ng/ml for plasma and 20.0 ng/g for brain. A limited pharmacokinetic analysis was performed on median values using WinNonlin™

Professional (Version-5.2.1). A non-compartmental analysis using the lin/log trapezoidal rule with lin/log interpolation was used for all data.

### **3 RESULTS:**

#### **3.1 PCP- and memantine-induced hyperlocomotion:**

##### **3.1.1. Acute dose-response testing:**

No significant differences in LMA were observed across study groups during the habituation phase ( $F(6,66) = 1.4$ ,  $p=ns$ ) [Table 3 (see suppl. material)]. Subsequent administration of PCP (0.63, 1.25 and 2.5 mg/kg SC) revealed a statistically significant increase versus vehicle treatment ( $F(3,38) = 8.5$ ,  $p<0.001$ ) where only the 2.5 mg/kg dose of PCP showed statistical significance ( $p = 0.004$ ). Memantine (10, 20 and 40 mg/kg IP) showed increased LMA at 20 and 40 mg/kg versus solvent [ $F(3,37)=11.3$ ,  $p<0.001$ ; Dunnett post hoc  $p=0.001$ ] [Table 3 (see suppl. material)]. The effect of the 40 mg/kg dose did not exceed the 20 mg/kg dose, probably due to stereotypic behaviour.

##### **3.1.2. Effect of sub-chronic PCP or memantine treatment on LMA:**

No differences were observed among treatment groups during the initial habituation phase [Table 4 (see suppl. material)]. Two-way ANOVA on the challenge phase data revealed a main effect for sub-chronic treatment ( $F(3,63) = 29.3$ ,  $p<0.001$ ) and for acute challenge ( $F(2,63) = 28.4$ ,  $p<0.001$ ) and also revealed an interaction for sub-chronic x acute challenge treatment( $F(1,63) = 6.4$ ,  $p=0.014$ ). Decomposition showed significant effects of acute memantine treatment in both sub-chronic memantine and sub-chronic vehicle treated subjects (both  $p<0.001$  for). The LMA-response to acute memantine administration in sub-chronic memantine or sub-chronic PCP treated rats was significantly higher than in the sub-chronic vehicle treated group ( $p<0.001$ ). Acute memantine administration to sub-chronic PCP treated rats also elicited a sensitized LMA-response ( $p<0.001$ ) [Table 4 (see suppl. material)].

##### **3.1.3. Effect of antipsychotic drugs on LMA in sub-chronic memantine treated rats:**

Memantine-induced hyperlocomotion was dose-dependently reversed by pre-treatment with classical antipsychotic drugs (see suppl. material).

### 3.2 Pharmacological MRI post acute and sub-chronic memantine treatment

**Voxel based analysis:** An acute dose of memantine (20 and 40 mg/kg IP) produced dose-dependent localized signal increases and decreases in the pre-limbic cortex of the brain (for a corrected  $p<0.05$ ,  $T=4.42$ , and  $p<0.05$ ,  $T=4.44$  respectively) [Figure 2 (a, b)]. Following sub-chronic memantine treatment of 20 mg/kg, i.p., significantly localized negative BOLD effects in the hippocampus, cingulate, pre-limbic and retrosplenial cortices were observed (for a corrected  $p<0.05$ ,  $T=4.44$ ) [Figure 2 (c)].

**Systemic effects:** To evaluate the confounding nature of the systemic effects within the statistical model the significance of the covariance of the global muscle signal intensities with the experimental paradigm (the injection protocol) were determined in each treatment group (Lowe et al. 2008). The outcome revealed a non-significant covariance with the paradigm (acute memantine 20 mg/kg { $F=1.187$ ,  $p=0.295$ }; acute memantine 40 mg/kg { $F=1.137$ ,  $p=0.197$ }; sub-chronic memantine 20 mg/kg { $F=3.022$ ;  $p=0.101$ }), hence the muscle signal intensity changes within these groups may justifiably be regarded as additive nuisance components within the model and not as a confound (Lowe et al. 2008; Sekar et al. 2011 (a, b)).

### 3.3 Resting state fMRI following sub-chronic memantine treatment

Brain regions which showed phMRI functional alterations after memantine treatment were used in a regional analysis of FC changes before and after sub-chronic memantine treatment (Figure 3). Decreases in FC were apparent amongst the hippocampus - pre-limbic cortex ( $F(1,6)=8.335$ ,  $p= 0.0028$ ), hippocampus - cingulate cortex ( $F(1,6)=8.314$ ,  $p= 0.0028$ ) and amongst the cortex (cingulate cortex – prelimbic cortex; ( $F(1,6)=8.013$ ,  $p= 0.030$ )). FC between left and right striatum (calculated as a negative control; no phMRI change expected) did not reflect a significant change upon subchronic memantine treatment ( $p=0.876$ ).

### 3.4 Diffusion MRI following sub-chronic memantine treatment and wash-out

Diffusion parameters including MK, RK, AK, MD, RD, AD, and FA were extracted from key ROIs (led by phMRI activations: including hippocampus, cingulate, pre-limbic and retrosplenial cortex) and striatum (control region). Statistical tests were conducted across the absolute

diffusion parameter values of the pre-treatment, post-treatment and post-washout datasets (Figure 4, 5).

The outcome of repeated measures ANOVA revealed statistical significant changes of the FA and AD in the hippocampus ( $F(2, 12) = 4.965, p=0.027$ ) and ( $F(2, 12) = 4.665, p=0.032$ ) respectively. Further AD values from the cingulate cortex also reflected significant changes ( $F(2, 12) = 4.604, p=0.033$ ). The rest of the diffusion parameters across all the regions of interest investigated failed to reflect any statistical significant change.

The paired sample t-test amongst the pre-treatment and post-treatment reflected significant decreases in the FA and AD in the hippocampus: ( $t(7, 2.43) = 2.953, p=0.021$ ) and ( $t(7, 7.22) = 2.79, p=0.027$ ) respectively; as well as marginally increase for the AD between the post-treatment and post-washout condition ( $t(3, 3.66) = -2.278, p=0.052$ ). Regarding the cingulate cortex, a statistical significant decrease was observed in the AD between pre- and post-treatment: ( $t(7, 6.2) = 2.796, p=0.027$ ).

### 3.5 Pharmacokinetics of memantine

Pharmacokinetics of memantine (20 mg/kg, IP) in plasma and brain revealed similar exposures (with comparable brain/plasma ratios) between acute and sub-chronic treatment (Figure 6). This result validates that the sub-chronic MRI responses being observed are not a result of differences in drug exposure, but due to the repeated sub-chronic treatment.

## 4 DISCUSSION:

There is strong preclinical and clinical evidence that NMDA receptor hypofunction models symptoms observed in schizophrenia. We aimed to map the neuroanatomical sites that are involved in the induction of NMDA-mediated changes using neuroimaging methods on rats. Our findings demonstrate the central effects of the non-competitive NMDA receptor antagonist memantine on brain activation, functional adaptations between acute vs. sub-chronic treatment, as well as its effect after sub-chronic treatment on brain functional connectivity and ultra-structural tissue integrity in rats.

Memantine-induced hyperlocomotion in naive and sub-chronically treated rats and its reversal by typical and atypical antipsychotic drugs in the present study is consistent with literature data

describing hyperlocomotion triggered by psychotropic stimulants in rodents (Nagai T, et al., 2003; Hackler et al. 2010; Ver Donck et al. 2011). This therefore validates the memantine model towards modelling NMDA mediated psychosis. Acute memantine-induced hyperlocomotion was further enhanced in rats previously treated sub-chronically for 5 days with memantine. This hypersensitisation to NMDA-antagonism is consistent with our earlier findings using sub-chronic PCP-treatment (Ver Donck et al, unpublished). Interestingly, reversal of memantine-induced hyperlocomotion by antipsychotic drugs in sub-chronic memantine treated rats was observed at doses that did not interfere with spontaneous locomotor activity.

Neuroanatomical target sites of drug action can be mapped using phMRI (Sekar et al. 2011 (a,b)). Acute doses of memantine induced dose-dependent and mainly negative BOLD phMRI responses, primarily in the pre-limbic cortex. The observed phMRI acute effects diverge from other studies in the direction of the changes (negative BOLD versus positive BOLD) after acute administration of NMDA-antagonists such as PCP, ketamine or MK801 (Gozzi et al. 2008-b; Hackler et al. 2010; Littlewood et al. 2006-a,b). Moreover Dedeurwaerdere et al. (2011) reported a robust increase in brain glucose metabolism after acute memantine treatment in mice, comparable to acute administration of other NMDA antagonists like ketamine. Compared to a single acute memantine dose, sub-chronic pre-treatment with memantine for 5 days resulted in more wide-spread negative BOLD. The difference observed between acute and sub-chronic memantine administration cannot be attributed to differences in plasma and brain exposure as we demonstrated similar pharmacokinetics after acute and sub-chronic treatment (Figure 6). In line with these results, most imaging studies find decreased brain activation in rodents and primates following sub-chronic NMDA antagonist treatment (Cochran et al. 2003; Dawson et al. 2010; Yu et al. 2011). Of note, a negative BOLD response would not necessarily reflect a concomitant decrease in neuronal activity, but could potentially reflect large increases in neuronal activity (Kastrup et al. 2008; Schridde et al, 2008). Though this finding would partially explain the increased brain glucose metabolism reported above, BOLD results are to be interpreted with caution. Our results showing involvement of additional brain regions following sub-chronic vs. acute treatment may indicate that priming the brain with repeated memantine injections, may sensitise the brain for a subsequent injection. The pre-limbic, cingulate, retrosplenial cortices and the hippocampus were identified as regions of drug action after sub-chronic memantine

treatment. These are potentially vulnerable regions in schizophrenia and are known to be involved in the mediation of cognitive functions in the domains affected in schizophrenia (Tamminga et al. 2006; Williamson & Allman 2012).

Recent studies indicate rs-fMRI to be an effective tool to study the functional signalling pathways in the brain (Jonckers et al. 2011; Krienen & Buckner 2009). Kurtosis MRI on the other hand indicates structural modifications in tissue integrity (Kyriakopoulos & Frangou 2009). The regions identified by the sub-chronic phMRI experiment were used as primary regions of interest for analysis in the subsequent resting-state functional connectivity and diffusion kurtosis MRI investigations. This includes the hippocampus, pre-limbic and cingulate cortices. Ample clinical evidence demonstrates disrupted functional connectivity within these circuits with rs-fMRI (Meyer-Lindenberg et al. 2005; Lawrie et al. 2002) and EEG studies (Ford et al. 2002) in schizophrenic patients. Following sub-chronic memantine treatment, there was a significantly decreased resting state FC between the hippocampus and the pre-limbic and cingulate cortices. Moreover, decreased FC was also apparent amongst the latter two brain regions. Recently, impaired hippocampal-prefrontal synchrony has been documented in a genetic mouse model of schizophrenia (Sigurdsson et al. 2010).

Clinical studies in schizophrenic patients have reported fractional anisotropy (FA) reductions (White et al. 2007). With diffusion kurtosis MRI we demonstrated that FA was affected in the hippocampus in particular, and axial diffusivity (AD) was significantly decreased in the hippocampus and cingulate cortex after sub-chronic memantine treatment. Moreover, these decreases in FA and AD persisted after a wash-out period of three days, indicating the long lasting nature of these diffusion changes. Our DKI results potentially suggest ultra-structural alterations in the hippocampus and the cingulate cortex after five days of sub-chronic memantine treatment at high dose. Whether these structural changes involve axonal degeneration, loss of synapses, oedema, or other changes would require further verification (Budde et al. 2011).

The level of anaesthesia used (i.e., 0.9 to 2% isoflurane) could be a potential confounding factor as it has been demonstrated that changes in anaesthesia can alter the direction of the BOLD response induced by NMDA antagonists (Gozzi et al. 2008-a). Therefore, the results are to be

interpreted with caution. However, immobilization of animals during scanning by anaesthesia is still considered the standard method to avoid motion artefacts and the influence of altered stress levels, which can lead to false positive activation. . While the study by Gozzi and colleagues (2008-a) suggested 0.8% of halothane anaesthesia as a cut-off, other studies using PCP (Hackler et al, 2010) or ketamine (Littlewood et al. 2006-a) in combination with isoflurane (1 and 1.6%, respectively) still obtained positive BOLD responses. Though the vast majority of MRI studies are still conducted under anaesthesia, imaging studies in conscious rodents are being endeavoured (Chin et al. 2011; Ling et al. 2011), using dedicated animal holder and acclimation training (King et al. 2005). Such approaches may hold promise for future rodent imaging.

Our multimodal imaging results provide evidence of concurrent decreases in BOLD signal, functional disconnectivity and altered ultra-structural tissue integrity in the prefrontal - hippocampal regions upon sub-chronic memantine treatment. This would substantiate the hypothesis that repeated NMDA receptor blockade with non-specific, non-competitive NMDA antagonists may lead to structural alterations particularly in the hippocampus and cingulate cortex. This study also illustrates the utility of comprehensive multimodal imaging (pharmacological, resting state and diffusion kurtosis MRI) towards the development of non-invasive imaging models.

In addition, it is important to note that memantine is a clinically approved drug, in contrast to its scheduled counterparts such as ketamine or PCP. Therefore, the use of memantine as a pharmacological challenge model carries a translational potential, as it would be possible to study the effects of memantine in man in well controlled imaging studies, both following acute and chronic/repeated administration.

**Conflict of interest:** The authors declare no conflict of interest.

**ACKNOWLEDGEMENT:** Financial support of Janssen Research & Development, Beerse, Belgium [Postdoctoral fellowship of Dr. Sekar]. The research leading to these results has received funding from the European Union's Seventh Framework Programme (FP7/2007-2013) under grant agreement no HEALTH-F2-2011-278850 (INMiND). Prof. Van der Linden and Prof. Dedeurwaerdere received funds from Fonds Wetenschappelijk Onderzoek Vlaanderen (FWO) (G.0586.12). Contributions of Mrs. Hilde Duytschaever, Mr. Patrick De Haes and Mr. Michel Mahieu, Mrs. Sofie Embrechts and Mrs. Liesbeth Mertens from Neuroscience Discovery, Janssen Research and Development for their support with the sub-chronic treatments and in generating the locomotor activity data are acknowledged. Results from this multimodal imaging study have been presented in part as abstracts at conferences including FlandersBio (2011), CINP Pacific Asia meet (2011), EMIM (2011) & WMIC (2011).

**REFERENCES:**

- Areosa SA, Sherriff F, McShane R (2005): Memantine for dementia. *The cochrane database for systematic reviews*. CD 003154.pub3. 2005
- Bifone A, Gozzi A, Schwarz AJ (2010): Functional connectivity in the rat brain: a complex network approach. *Magn Reson Imaging* 28(8): 1200-9. (Review)
- Borsook D, Becerra L, and Hargreaves R (2006): A role for fMRI in optimizing CNS drug development. *Nat Rev Drug Discov* 5:411-424.
- Borsook D, Becerra L (2010): Using NMR approaches to drive the search for new CNS therapeutics. *Curr Opin Investig Drugs* 11(7): 771-8. (Review)
- Bubeníková-Valesová V, Horácek J, Vrajová M, Höschl C (2008): Models of schizophrenia in humans and animals based on inhibition of NMDA receptors. *Neurosci Biobehav Rev* 32(5): 1014-23. Epub 2008 Apr 8. (Review)
- Budde MD, Janes L, Gold E, Turtzo LC, Frank JA (2011): The contribution of gliosis to diffusion tensor anisotropy and tractography following traumatic brain injury: validation in the rat using Fourier analysis of stained tissue sections. *Brain* 134(Pt 8):2248-60.
- Chin CL, Upadhyay J, Marek GJ, Baker SJ, Zhang M, Mezler M, Fox GB, Day M (2011): Awake Rat Pharmacological Magnetic Resonance Imaging as a Translational Pharmacodynamic Biomarker: Metabotropic Glutamate 2/3 Agonist Modulation of Ketamine-Induced Blood Oxygenation Level Dependence Signals *J Pharmacol Exp Ther*. 336(3):709-15
- Cochran SM, Kennedy M, McKerchar CE, Steward LJ, Pratt JA, Morris BJ (2003): Induction of metabolic hypofunction and neurochemical deficits after chronic intermittent exposure to phencyclidine: differential modulation by antipsychotic drugs. *Neuropsychopharmacology* 28(2):265-75.
- Coyle JT, Tsai G. (2004): NMDA receptor function, neuroplasticity, and the pathophysiology of schizophrenia. *Int Rev Neurobiol* 59: 491-515. (Review)
- Danysz W, Parsons CG, Mobius HJ, Stoffler A, Quack G (2000): Neuroprotective and symptomatological action of memantine relevant for Alzheimer's disease – A unified glutamatergic hypothesis on the mechanism of action. *Neurotox Res* 2(2-3): 85-97.
- Dawson N, Thompson RJ, McVie A, Thomson DM, Morris BJ, Pratt JA (2010): Modafinil Reverses Phencyclidine-Induced Deficits in Cognitive Flexibility, Cerebral Metabolism, and Functional Brain Connectivity. *Schizophr bull* Sep 1. [Epub ahead of print].
- Dedeurwaerdere S, Wintmolders C, Straetemans R, Pemberton D, Langlois X (2011): Memantine-induced brain activation as a model for the rapid screening of potential novel antipsychotic compounds: exemplified by activity of an mGlu2/3 receptor agonist. *Psychopharmacology* 214: 505-514.
- Delgado y Palacios R, Campo A, Henningsen K, Verhoye M, Poot D, Dijkstra J, Van Audekerke J, Benveniste H, Sijbers J, Wiborg O, Van der Linden A (2011): Magnetic resonance imaging and spectroscopy reveal differential hippocampal changes in anhedonic and resilient subtypes of the chronic mild stress rat model. *Biol Psychiatry* 70(5): 449-57
- Ford JM, Mathalon DH, Whitfield S, Faustman WO, Roth WT (2002): Reduced communication between frontal and temporal lobes during talking in schizophrenia. *Biol Psychiatry* 51(6): 485-92.
- Fox GB, Chin CL, Luo F, Day M, and Cox BF (2009): Translational neuroimaging of the CNS: novel pathways to drug development. *Mol Interv* 9: 302–313.
- Gilmour G, Pioli EY, Dix SL, Smith JW, Conway MW, Jones WT, Loomis S, Mason R, Shahabi S, Tricklebank MD. (2009): Diverse and often opposite behavioral effects of NMDA receptor antagonists in rats: implications for “NMDA antagonist modelling” of schizophrenia. *Psychopharmacology* 205: 203–216.
- Gozzi A, Herdon H, Schwarz A, Bertani S, Crestan V, Turrini G, Bifone A (2008-a): Pharmacological stimulation of NMDA receptors via co-agonist site suppresses fMRI response to phencyclidine in the rat. *Psychopharmacology (Berl)* 201(2): 273-84.

Gozzi A, Large CH, Schwarz A, Bertani S, Crestan V, Bifone A (2008-b): Differential effects of antipsychotic and glutamatergic agents on the phMRI response to phencyclidine. *Neuropsychopharmacology* 33(7): 1690-703.

Hackler EA, Byun NE, Jones CK, Williams JM, Baheza R, Sengupta S, Grier MD, Avison M, Conn PJ, Gore JC (2010): Selective potentiation of the metabotropic glutamate receptor subtype 2 blocks phencyclidine-induced hyperlocomotion and brain activation. *Neuroscience* 168(1):209-18.

Hlustik P, Noll DC, Small SL (1998): Suppression of vascular artifacts in functional magnetic resonance images using MR angiograms. *Neuroimage* 7: 224-231.

Houston GC, Papadakis NG, Carpenter TA, Hall LD, Mukherjee B, James MF, Huang CL (2001): Mapping of brain activation in response to pharmacological agents using fMRI in the rat. *Magn Reson Imaging* 19(7): 905-19.

Jensen JH, Helpern JA, Ramani A, Lu H, Kaczynski K (2005): Diffusional kurtosis imaging: the quantification of non-gaussian water diffusion by means of magnetic resonance imaging. *Magnetic resonance in medicine* 53(6): 1432-40.

Jonckers E, Van Audekerke J, De Visscher G, Van der Linden A, Verhoye M (2011): Functional connectivity fMRI of the rodent brain: comparison of functional connectivity networks in rat and mouse. *PLoS One* 6(4):e18876.

Kalthoff D, Seehafer JU, Po C, Wiedermann D, Hoehn M (2011): Functional connectivity in the rat at 11.7T: Impact of physiological noise in resting state fMRI. *Neuroimage* 54(4): 2828-39.

Kastrup A, Baudewig J, Schnaudigel S, Huonker R, Becker L, Sohns JM, Dechent P, Klingner C, Witte OW (2008): Behavioral correlates of negative BOLD signal changes in the primary somatosensory cortex. *Neuroimage* 41(4): 1364–1371.

Krienen FM, Buckner RL (2009): Segregated fronto-cerebellar circuits revealed by intrinsic functional connectivity. *Cereb Cortex* 19(10): 2485-97.

Krystal JH, Karper LP, Seibyl JP, Freeman GK, Delaney R, Bremner JD, Heninger GR, Bowers MB Jr, Charney DS (1994) Subanesthetic effects of the noncompetitive NMDA antagonist, ketamine, in humans. Psychotomimetic, perceptual, cognitive, and neuroendocrine responses. *Arch Gen Psychiatry* 51:199–214.

Kyriakopoulos M, Frangou S (2009): Recent diffusion tensor imaging findings in early stages of schizophrenia. *Current Opinion in Psychiatry* 22: 168–176.

Langsjo JW, Kaisti KK, Aalto S, Hinkka S, Aantaa R, Oikonen V, Sipilä H, Kurki T, Silvanto M, Scheinin H. (2003): Effects of subanesthetic doses of ketamine on regional cerebral blood flow, oxygen consumption, and blood volume in humans. *Anesthesiology* 99(3): 614-23.

Langsjo JW, Salmi E, Kaisti KK, Aalto S, Hinkka S, Aantaa R, Viljanen T, Kurki T, Silvanto M, Scheinin H. (2004): Effects of subanesthetic ketamine on regional cerebral glucose metabolism in humans. *Anesthesiology* 100(5): 1065-71.

Lawrie SM, Buechel C, Whalley HC, Frith CD, Friston KJ, Johnstone EC (2002): Reduced frontotemporal functional connectivity in schizophrenia associated with auditory hallucinations. *Biol Psychiatry* 51(12): 1008-11.

Leemans A, Jones DK (2009): The B-matrix must be rotated when correcting for subject motion in DTI data. *Magnetic resonance in medicine* 61(6): 1336-49.

Ling Z, King JA, Zhang N. (2011): Uncovering Intrinsic Connectional Architecture of Functional Networks in Awake Rat Brain. *The Journal of Neuroscience* 31(10):3776 –3783. PMID: 21389232

Littlewood CL, Jones N, O'Neill MJ, Mitchell SN, Tricklebank M, Williams SC (2006-a): Mapping the central effects of ketamine in the rat using pharmacological MRI. *Psychopharmacology (Berl)* 186(1): 64-81.

Littlewood CL, Cash D, Dixon AL, Dix SL, White CT, O'Neill MJ, Tricklebank M, Williams SC (2006-b): Using the BOLD MR signal to differentiate the stereoisomers of ketamine in the rat. *Neuroimage* 32(4): 1733-46.

Lowe AS, Barker GJ, Beech JS, Ireland MD, Williams SC (2008): A method for removing global effects in small-animal functional MRI. *NMR Biomed* 21: 53-58.

Maes F, Collignon A, Vandermeulen D, Marchal G, Suetens P (1997): Multimodality image registration by maximization of mutual information. *IEEE transactions on Medical Imaging* 16(2): 187-198.

Malhotra AK, Pinals DA, Adler CM, Elman I, Clifton A, Pickar D, and Breier A (1997) Ketamine-induced exacerbation of psychotic symptoms and cognitive impairment in neuroleptic-free schizophrenics. *Neuropsychopharmacology* 17:141–150.

Mechri A, Micallef J, Blin O, Saoud M, Daléry J, Gaha L (2001-a): Pharmacological modulation of the effects induced by ketamine at subanesthetic doses. *Therapie* 56(5): 617-22 (Review)

Mechri A, Saoud M, Khiari G, d'Amato T, Daléry J, Gaha L (2001-b): Glutaminergic hypothesis of schizophrenia: clinical research studies with ketamine. *Encephale* 27(1): 53-9. (Review)

Meyer-Lindenberg AS, Olsen RK, Kohn PD, Brown T, Egan MF, Weinberger DR, Berman KF. (2005): *Arch Gen Psychiatry* 62(4): 379-86.

Nagai, T., Noda, Y., Une, T., Furukawa, K., et al. (2003) Effect of AD-5423 on animal models of schizophrenia: phencyclidine-induced behavioral changes in mice. *Neuroreport* 14, 269–272.

Olney, J.W., Farber, N.B., (1995): NMDA antagonists as neurotherapeutic drugs, psychotogens, neurotoxins, and research tools for studying schizophrenia. *Neuropsychopharmacology* 13, 335-345.

Olney, J.W., Labruyere, J., Wang, G., Wozniak, D.F., Price, M.T., Sesma, M.A., (1991): NMDA antagonist neurotoxicity: mechanism and prevention. *Science* 254, 1515-1518.

Peskind ER, Potkin SG, Pomara N, Ott BR, Graham SM, Olin JT, McDonald S (2006): Memantine Treatment in Mild to Moderate Alzheimer Disease: A 24-Week Randomized, Controlled Trial. *Am J Geriatr Psychiatry* 14 (8): 704 - 715.

Parsons CG, Stoffler A, Danysz W (2007): Memantine: a NMDA receptor antagonist that improves memory by restoration of homeostasis in the glutamatergic system - too little activation is bad, too much is even worse. *Neuropharmacology* 53: 699–723.

Pawela CP, Biswal BB, Hudetz AG, Schulte ML, Li R, Cho YR, Matloub HS, Hyde JS (2009): A protocol for use of medetomidine anesthesia in rats for extended studies using task-induced BOLD contrast and resting-state functional connectivity. *Neuroimage* 46:1137–1147.

Schwarz AJ, Gozzi A, Reese T, Heidbreder CA, Bifone A (2007): Pharmacological modulation of functional connectivity: the correlation structure underlying the phMRI response to d-amphetamine modified by selective dopamine D3 receptor antagonist SB277011A. *Magn Reson Imaging* 25(6): 811-20.

Schriddé U, Khubchandani M, Motelow JE, Sanganahalli BG, Hyder F, Blumenfeld H (2008): Negative BOLD with large increases in neuronal activity. *Cerebr Cortex* 18(8): 1814–1827.

Sekar S, Raley JM, Lowe AS, Sharp T, Sibson NR, Blamire AM, Steckler T, Shoaib M (2010): Mapping of anxiogenic neuronal profiles induced by the GABA inverse agonist FG-7142 and caffeine using pharmacological magnetic resonance imaging. *European Neuropsychopharmacology* 20(1): S23

Sekar S, Verhoye M, Van Audekerke J, Vanhoutte G, Lowe AS, Blamire AM, Steckler T, Van der Linden A, Shoaib M. (2011-a): Neuroadaptive responses to citalopram in rats using pharmacological magnetic resonance imaging. *Psychopharmacology (Berl)* 213: 521-531

Sekar S, Van Audekerke J, Vanhoutte G, Lowe AS, Blamire AM, Van der Linden A, Steckler T, Shoaib M, Verhoye M. (2011-b): Neuroanatomical targets of reboxetine and bupropion as revealed by pharmacological magnetic resonance imaging. *Psychopharmacology (Berl)* 217(4):549-57.

Sigurdsson T, Stark KL, Karayiorgou M, Gogos JA, Gordon JA (2010): Impaired hippocampal-prefrontal synchrony in a genetic mouse model of schizophrenia. *Nature* 464(7289): 763-7.

Tamminga CA (2006): The neurobiology of cognition in schizophrenia. *J Clin Psychiatry*. 67 Suppl 9:9-13; discussion 36-42.

Van Hecke W, Sijbers J, D'Agostino E, Maes F, De Backer S, Vandervliet E, Parizel PM, Leemans A (2008): On the construction of an inter-subject diffusion tensor magnetic resonance atlas of the healthy human brain. *NeuroImage* 43(1): 69-80.

Veraart J, Poot DH, Van Hecke W, Blockx I, Van der Linden A, Verhoye M, Sijbers J (2011): More accurate estimation of diffusion tensor parameters using diffusion Kurtosis imaging. *Magnetic resonance in medicine* 65(1): 138-45.

Ver Donck L, Duytschaever H, Willemse R (2011): Low dose subchronic phencyclidine (PCP) pretreatment potentiates acute PCP-induced hyperlocomotion in adult rats: a model of schizophrenia? *Society for Neuroscience*, abstract 368.13.

Weber R, Ramos-Cabrer P, Wiedermann D, van Camp N, Hoehn M (2006): A fully noninvasive and robust experimental protocol for longitudinal fMRI studies in the rat. *Neuroimage* 29: 1303-1310.

White T, Kendi AT, Lehericy S, Kendi M, Karatekin C, Guimaraes A, Davenport N, Schulz SC, Lim KO (2007): Disruption of hippocampal connectivity in children and adolescents with schizophrenia - A voxel-based diffusion tensor imaging study. *Schizophrenia Research* 90: 302-307.

Winblad B, Jones RW, Wirth Y, Stöffler A, Möbius HJ (2007): Memantine in Moderate to Severe Alzheimer's Disease: A Meta-Analysis of Randomised Clinical Trials. *Dementia and Geriatric Cognitive Disorders* 24: 20-27.

Wilcock G, Mobius HJ, Stoffler A (2002): A double-blind, placebo-controlled multicentre study of memantine in mild to moderate vascular dementia. *Int Clin Psychopharmacol* 17:297-305.

Williamson PC, Allman JM (2012): A framework for interpreting functional networks in schizophrenia. *Front Hum Neurosci*. 6:184

Williams KA, Magnuson M, Majeed W, Laconte SM, Peltier SJ, Keilholz SD. (2010): Comparison of alpha-chloralose, medetomidine and isoflurane anesthesia for functional connectivity mapping in the rat. *Magn Reson Imaging*. 28:995-1003

Wong DF, Tauscher J, and Grunder G (2009): The role of imaging in proof of concept for CNS drug discovery and development. *Neuropsychopharmacology* 34:187-203

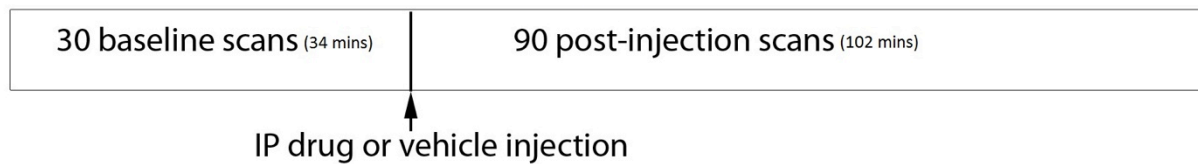
Yu H, Li Q, Wang D, Shi L, Lu G, Sun L, Wang L, Zhu W, Mak YT, Wong N, Wang Y, Pan F, Yew DT. (2011): Mapping the central effects of Chronic ketamine administration in an adolescent primate model by functional magnetic resonance imaging(fMRI). *Neurotoxicology* 33(1):70-77

**Table 2: Study design and overview of the MRI experiments**

Type of MRI modality	Treatment & dose	Number of subjects	Experimental design (longitudinal scanning)
<b>phMRI</b>	Acute memantine or vehicle (20 or 40 mg/kg, IP) treatment	6 per group	Individual groups (n = 3)
<b>phMRI</b>	Sub-chronic memantine or vehicle (20 mg/kg, IP/day - 5 days) treatment	6 per group	Individual groups (n = 2)
<b>rs-fMRI</b>	Sub-chronic memantine (20 mg/kg, IP/day - 5 days) treatment	8 subjects	Same subject group scanned at 2 time-points (pre & post treatment)
<b>DKI</b>	Sub-chronic memantine (20 mg/kg, IP/day - 5 days) treatment	10 subjects	Same subject group scanned at 3 time-points (pre & post treatment and post 3 days washout)

phMRI: pharmacological MRI; rs-fMRI: resting state functional-MRI; DKI: Diffusion kurtosis imaging

## (a) phMRI scanning experimental design (120 functional scans; 1 scan = 1min 8 sec)



## (b) rs-fMRI or DKI (scanning timepoint's and treatment scheme)

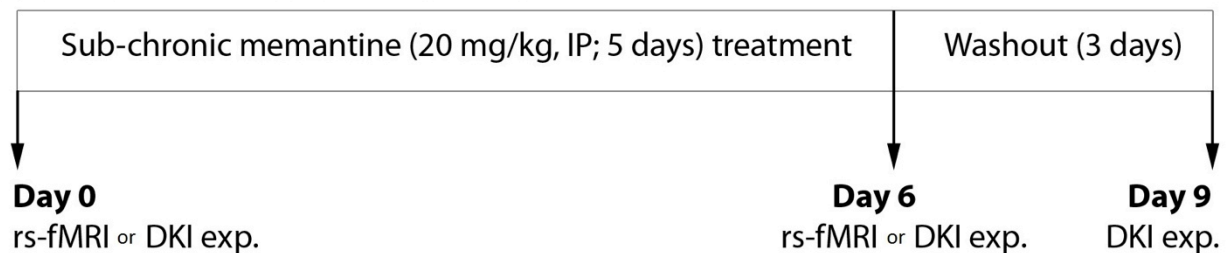


**Figure 1:Experimental protocol of phMRI-study (a) and rs-fMRI & DKI-study (b)**

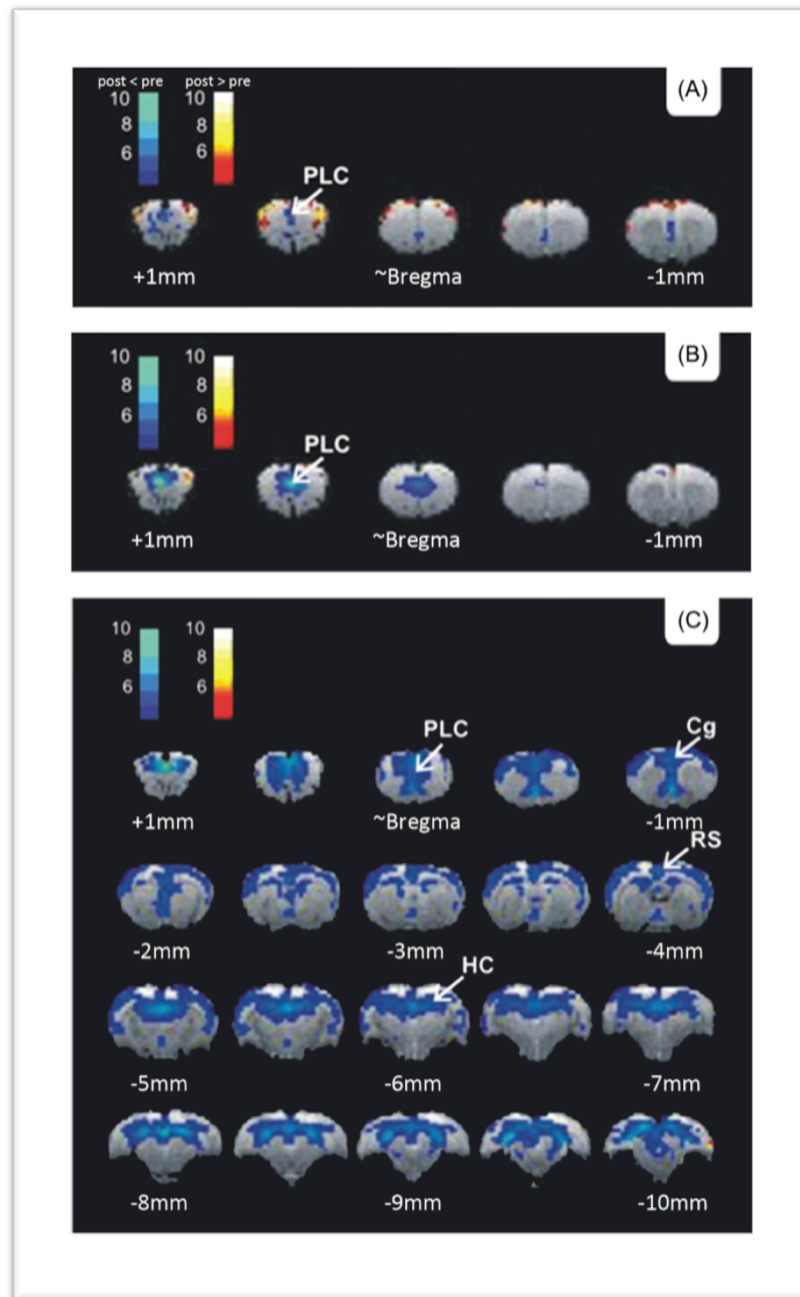


**Figure 2 - PhMRI Results:** SPM  $\{t\}$  distribution maps representing BOLD signal changes from memantine treated study groups overlaid on anatomical template image. Coloured pixels represent significant T-scores (threshold at  $p<0.05$  corrected for multiple comparisons) of signal time course with input test condition (pre- vs. post-test injection). Red and blue represent BOLD increase and decrease, respectively. (a)- Statistical significance of 20 mg/kg, IP acute memantine ( $T>4.42$ ). (b)- statistical significance of 40 mg/kg, IP, acute memantine ( $T>4.44$ ). (c)- Statistical significance of 20 mg/kg, IP, subchronic (5 days) memantine ( $T>4.44$ ).

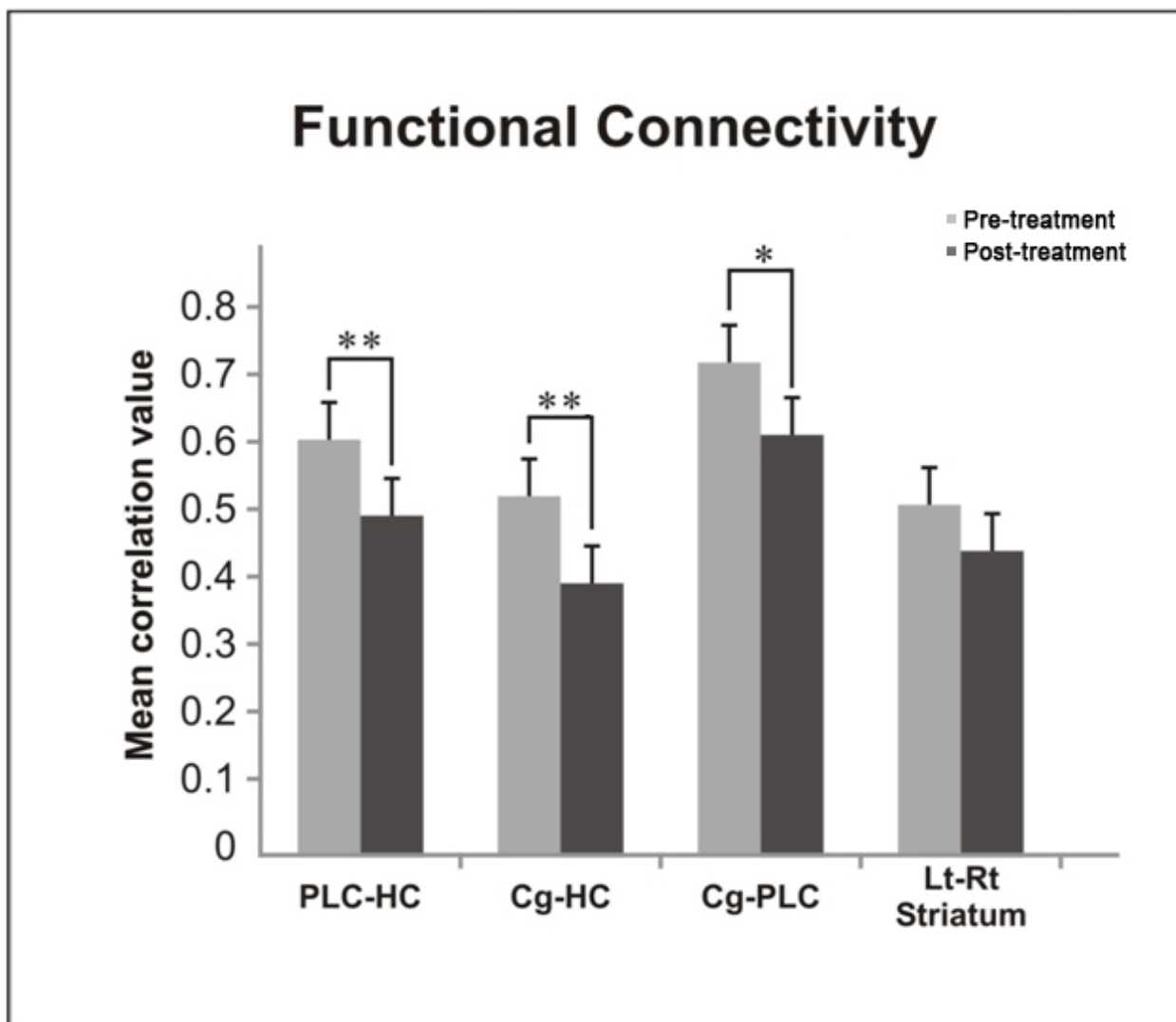


**Figure 4:** Resting state functional magnetic resonance imaging results reflecting the strength of functional connectivity between the regions before and after 20 mg/kg IP, sub-chronic memantine treatment. [PLC: pre-limbic cortex; Cg: cingulate cortex; HC: hippocampus; Lt-Rt Striatum: left - right striatum]. [\*\* ( $p<0.01$ ), \* ( $p<0.05$ ): level of significant difference between pre- versus post-treatment]

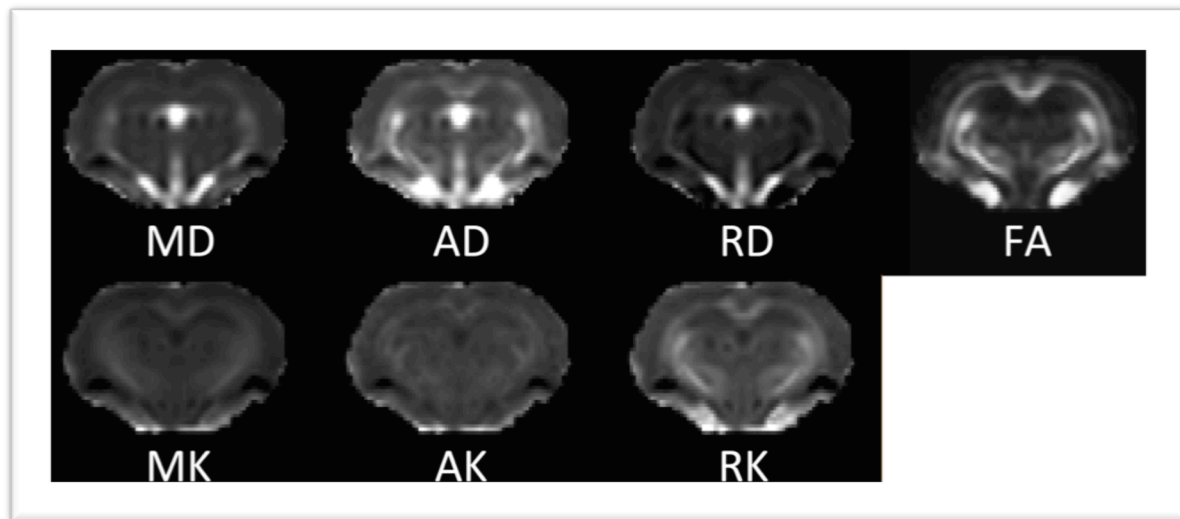


**Figure 4: DTI/DKI Map** [diffusion tensor parameters: axial- (AD), radial- (RD) & mean-diffusivity (MD); fractional anisotropy (FA) and diffusion kurtosis parameters: mean- (MK), axial- (AK) & radial-kurtosis (RK)]

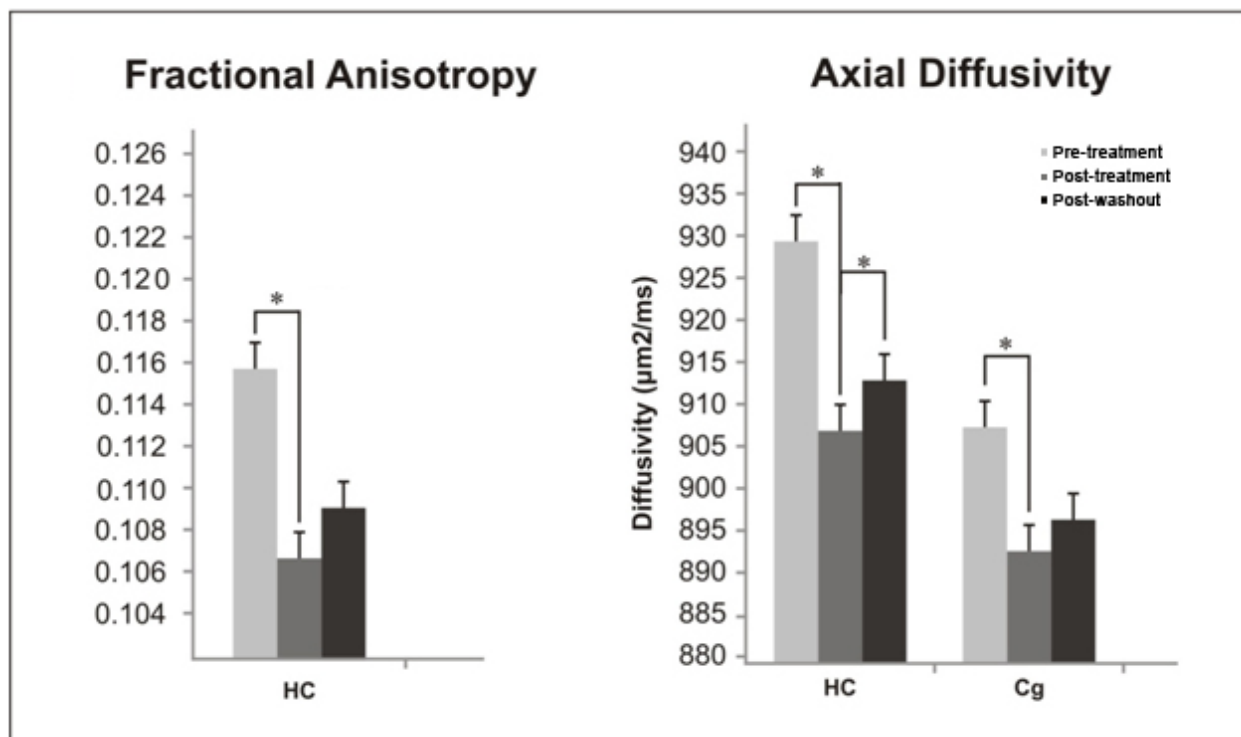


**Figure 5: Diffusion kurtosis magnetic resonance imaging results pre & post 20 mg/kg IP, sub-chronic memantine treatment and post washout.** [\* ( $p < 0.05$ ) level of significant difference]

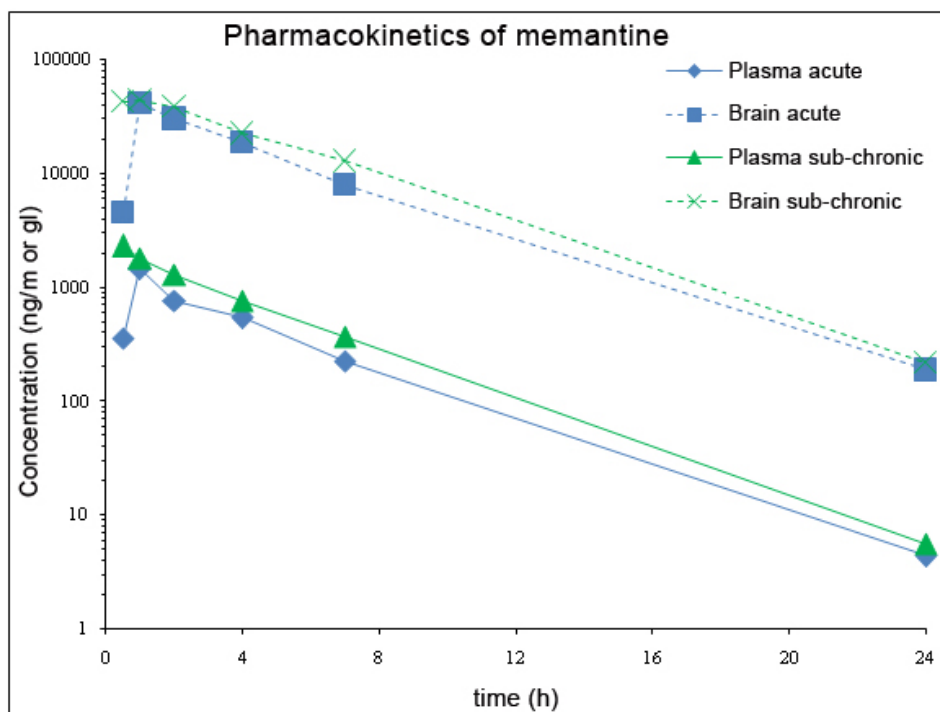


**Figure 6: Pharmacokinetics of memantine** at time points of 0.5, 1, 2, 4, 7 and 24 h post-injection (memantine 20mg/kg, IP); mean data are presented at each time point as n=3.